Human Molecular Genetics, 2009, Vol. 18, No. 6 **1099–1109**
doi:10.1093/hmg/ddp006
Advance Access published on January 15, 2009

Efhc1 deficiency causes spontaneous myoclonus and increased seizure susceptibility

Toshimitsu Suzuki[1,6], Hiroyuki Miyamoto[2], Takashi Nakahari[7], Ikuyo Inoue[1], Takahiro Suemoto[3], Bin Jiang[4], Yuki Hirota[8], Shigeyoshi Itohara[5], Takaomi C. Saido[3], Tadaharu Tsumoto[4], Kazunobu Sawamoto[8], Takao K. Hensch[2], Antonio V. Delgado-Escueta[9] and Kazuhiro Yamakawa[1,*]

[1]Laboratory for Neurogenetics, [2]Laboratory for Neuronal Circuit Development, [3]Laboratory for Proteolytic Neuroscience, [4]Tsumoto Research Unit, [5]Laboratory for Behavioral Genetics and [6]Special Postdoctoral Researchers Program, RIKEN Brain Science Institute (BSI), 2-1 Hirosawa, Wako-shi, 351-0198 Saitama, Japan, [7]Department of Physiology, Osaka Medical College, Osaka 569-8686, Japan, [8]Department of Developmental and Regenerative Biology, Institute of Molecular Medicine, Nagoya City University Graduate School of Medical Sciences, Nagoya 467-8601, Japan and [9]Epilepsy Genetics/Genomics Laboratories, Comprehensive Epilepsy Program, UCLA Geffen School of Medicine and VA GLAHS-West Los Angeles, Los Angeles, CA 90073, USA

Received November 6, 2008; Revised and Accepted December 23, 2008

Mutations in *EFHC1* gene have been previously reported in patients with epilepsies, including those with juvenile myoclonic epilepsy. Myoclonin1, also known as mRib72-1, is encoded by the mouse *Efhc1* gene. Myoclonin1 is dominantly expressed in embryonic choroid plexus, post-natal ependymal cilia, tracheal cilia and sperm flagella. In this study, we generated viable *Efhc1*-deficient mice. Most of the mice were normal in outward appearance, and both sexes were found to be fertile. However, the ventricles of the brains were significantly enlarged in the null mutants, but not in the heterozygotes. Although the ciliary structure was found intact, the ciliary beating frequency was significantly reduced in null mutants. In adult stages, both the heterozygous and null mutants developed frequent spontaneous myoclonus. Furthermore, the threshold of seizures induced by pentylenetetrazol was significantly reduced in both heterozygous and null mutants. These observations seem to further suggest that decrease or loss of function of myoclonin1 may be the molecular basis for epilepsies caused by *EFHC1* mutations.

INTRODUCTION

Juvenile myoclonic epilepsy (JME) is a common adolescent onset myoclonic, clonic-tonic-clonic (grand mal) generalized epilepsy (IGE) that is responsible for 3–12% of all known epilepsies (1–3). Electroencephalography (EEG) reveals 15–30 Hz multispikes during myoclonic and tonic-clonic convulsions. Moreover, 3.5–6 Hz multispikes and wave complexes appear in 17% of clinically asymptomatic members of JME families (1). We previously identified mutations in the *EFHC1* (EF-hand domain containing 1) gene that segregated with epilepsy and the appearance of EEG polyspike wave in patients of JME families (4). The human *EFHC1* encodes a 640 amino acid non-ion channel protein myoclonin1 that harbors three tandemly repeated DM10 domains, a motif of unknown function and one EF-hand calcium-binding motif at the C terminus. *EFHC1* mRNA was observed in multiple tissues, including the brain in northern blot analyses (4). We also previously reported along with another group that mouse myoclonin1 protein was dominantly expressed in choroid plexus at restricted developmental stages in the fetus and in the cilia of ependymal cells lining the wall of ventricles, tracheal cilia and sperm flagella at post-natal stages (5,6).

Successive studies by other groups have confirmed our findings by reporting a single *EFHC1* heterozygous missense mutation in one of 54 JME Caucasian families (7) and two missense mutations in two of 27 Italian JME families (8).

*To whom correspondence should be addressed. Tel: +81 484679703; Fax: +81 484677095; Email: yamakawa@brain.riken.jp

In addition to the mutations in JME, Stogmann *et al.* (9) previously described *EFHC1* mutations in other types of idiopathic epilepsies: three missense mutations in four patients with juvenile absence epilepsy, cryptogenic temporal lobe epilepsy (cTLE) and an unclassified IGE of 61 IGE (including 24 JME) and 372 TLE patients.

In addition to the original full-length myoclonin1, the *EFHC1* gene also encodes a short isoform of myoclonin1 (278 amino acids) that harbors only one DM10 domain without an EF-hand motif and a unique C-terminal end (4). We recently identified heterozygous frameshift and nonsense mutations in the part of *EFHC1* transcript encoding the unique C-terminal end of the myoclonin1 short isoform in three JME families (two families from Honduras and one from Mexico) as well as identified new missense mutations in the original long isoform of *EFHC1* in two JME families (from Mexico and Japan) (10).

Although the results of these familial studies have indicated that *EFHC1* mutations may be genetically responsible for the observed epilepsies, direct physiological or biological evidence have been rather scarce to date. To further address the putative relevance of *EFHC1* in epilepsies, we generated and characterized *Efhc1*-deficient mice. We found that disruption of *Efhc1* in mice caused frequent spontaneous myoclonus and enhanced seizure susceptibility to chemoconvulsant stimulation. Our findings further support the contention that *EFHC1* is a gene responsible for some forms of epilepsies.

RESULTS

Generation of *Efhc1*-deficient mouse

We constructed a targeting vector in which a phosphoglycerate kinase-promoted neomycin resistance gene cassette was inserted into exon 1 of the *Efhc1* gene (Fig. 1A). This caused a frameshift at amino acid position 14 of myoclonin1 and introduced a premature stop codon six amino acids further down from the frameshift. This frameshift effectively eliminated most of the *Efhc1* coding sequence, rendering it non-functional. Genotypes of targeted embryonic stem (ES) clones were verified by Southern blot analysis and polymerase chain reaction (PCR) (Fig. 1B and C). Mice carrying the targeted allele were derived from two independent ES clones and showed identical phenotypes. *Efhc1* homozygous mutant (null) and heterozygous offspring were viable and were produced in the expected Mendelian genotype ratio (~25 and ~50%, respectively). Reverse-transcriptase–PCR (RT–PCR) analyses of RNAs extracted from the brain, kidney and liver tissues revealed no *Efhc1* mRNA in the null mutants (Fig. 1D). Genotypes of the mice were determined by PCR using genomic DNA isolated from the tail (Fig. 1E). We previously reported the absence of myoclonin1 protein in the null mutants by western blot and immunohistochemical analyses using an anti-myoclonin1 monoclonal antibody (6A3-mAb) (5). Heterozygous and null mutants were fertile in both sexes and showed mostly normal growth with no gross abnormalities in their outward appearance. Although myoclonin1 is dominantly expressed in the sperm flagella and oviduct (6), the observed preserved fertility of the null mutant male and female mice suggests that the absence of myoclonin1 in the sperm flagellum and oviductal cilia does not adversely affect the motility and function of these structures.

Increased spontaneous myoclonus in both heterozygous and null *Efhc1*-deficient mice

The *Efhc1* mutant mice developed spontaneous recurrent involuntary movement of the whole body (muscular jerks) at 7–8 months of age (Fig. 2 and Supplementary Material, Video S1). Each episode of the jerks lasted for less than ~200 ms and usually consisted of one to three jerks with brief electromyographic bursts (positive myoclonus), with the mice immediately returning back to normal behavior after each of the episodes. Movements without electromyographic bursts were assumed to be voluntary ones and were not included in the count. The frequency of myoclonus was seven to eight times higher in the heterozygous and null mutants compared with the background level of wild-type littermates (Fig. 2B). These involuntary twitches and jerks (myoclonus) synchronously involved the whole body, simultaneously activating the upper body in the shoulders and head bilaterally, often propelling the mice backwards. These semiologies suggest an afferent volley outside the cerebral cortex and a pontobulbospinal activation. Jerks were observed during both the sleep and wake phases. A blind observer to the genotype readily detected these twitches by electromyogram (EMG). By using bilaterally implanted somatosensory cortex parietal electrodes, we monitored the electrocorticograms (EcoGs) in freely moving 7–8-month-old mice. We did not observe prominent abnormal EEG activity in the null or heterozygous mutants in each single measurement of myoclonus. However, the polygraphic analysis revealed that the back-averaging of evoked potentials in the EcoG recordings gave positive signals when triggered to involuntary movements (positive myoclonus) (Fig. 2C), but not when triggered to voluntary movements (Fig. 2D). These results may suggest that spontaneous myoclonus in the mutants is not cortical but may possibly be subcortical (thalamus, etc.) or perhaps brain stem in origin.

Increased seizure susceptibility to a chemoconvulsant stimulation in both heterozygous and null *Efhc1*-deficient mice

We next investigated the seizure susceptibility of the *Efhc1*-deficient mice by using chemoconvulsant, pentylenetetrazole (PTZ). PTZ, a gamma-aminobutyric acid (GABA) receptor α1 subunit antagonist, is one of the most commonly used pharmacological agents for inducing seizures (11). After intraperitoneal (i.p.) application of 50 mg/kg body weight of PTZ in 4–5-month and 9–12-month-old mice, a much larger number of the heterozygous and null mutant mice showed generalized convulsive seizures (GS) when compared with wild-type mice (Fig. 3). The latency until the onset of seizures was also significantly decreased in both the heterozygous and null mutants. We then further evaluated myoclonic jerks (MJs) and clonic seizures (CLs) (Supplementary Material, Fig. S1 and Fig. 3). Although MJs did not show significant differences among genotypes, more frequent CL with shorter latency was observed in both the mutants. When observed at

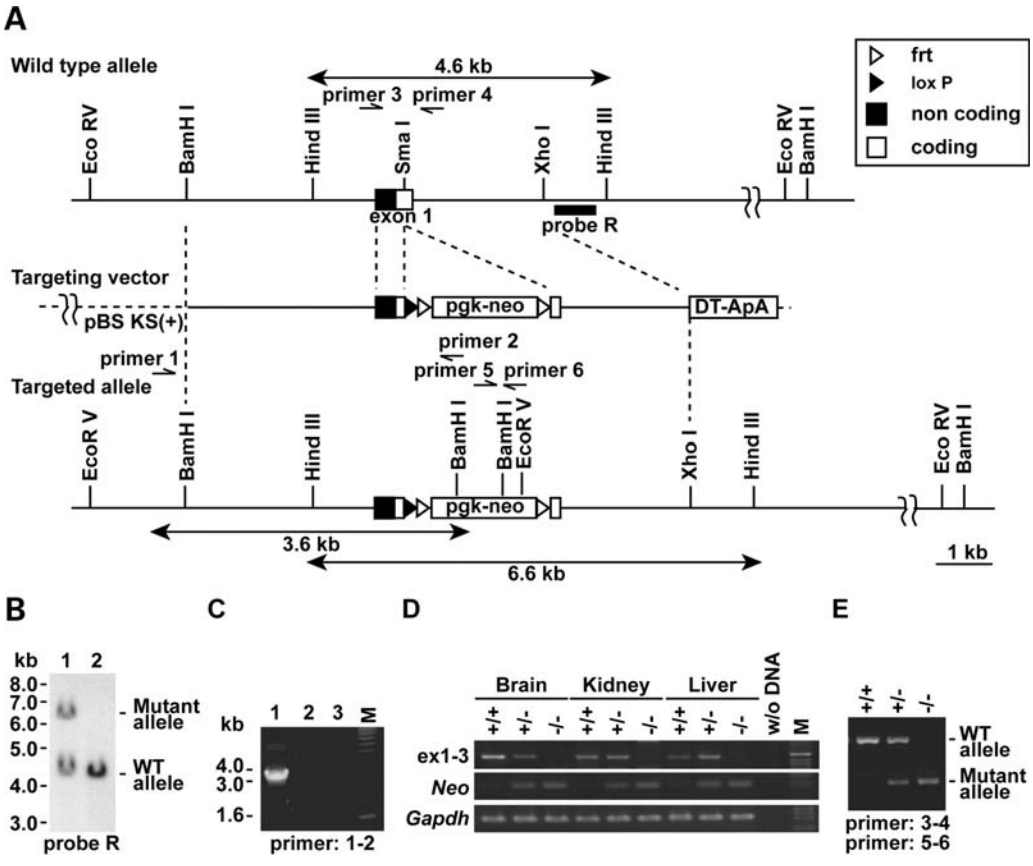

Figure 1. Generation of *Efhc1*-deficient mice. (**A**) Schematic diagram of *Efhc1* genomic sequence (top), targeting construct (middle) and targeted *Efhc1* allele (bottom). The coding (white box) and non-coding (blackened box) regions of exon 1 are shown. Relative position of the 3′ external probe (probe R) used to detect the targeted allele is shown under the wild-type allele. The predicted size of the wild-type (4.6 kb) and targeted (6.6 kb) alleles that probe R would detect in *Hin*dIII digests is shown. (**B**) Southern blot analysis of *Hin*dIII-digested genomic DNA from mouse ES cells. Probe R identified expected size fragments of wild-type and targeted mutant alleles. Lane 1 is targeted ES cell and lane 2 is wild-type ES cell. (**C**) Homologous recombination of left arm was confirmed by PCR. The PCR analysis, performed on genomic DNA derived from ES cells, resulted in the amplification of the expected size fragment in the homologous recombinant ES cell (lane 1), but not in the wild-type sample (lane 2). Lane 3 refers to the reaction without a template. (**D**) RT–PCR analysis for *Efhc1* mRNA expression in mutant mice. Primers on *Efhc1* cDNA (exon-connection PCR primer pair exon 1F/exon 3R) or on *pgk-neo* (Neo) cDNA (primer pair primer 5/primer 6) were designed to amplify 462 bp fragment from the *Efhc1* cDNA or 152 bp fragment from the *Neo* cDNA. The RT–PCR analysis, performed on cDNAs derived from brain, kidney and liver total RNA, resulted in amplification of the expected size *Efhc1* exons 1–3 fragment in the wild-type (+/+) and heterozygous (+/−) but not in the homozygous null mutant (−/−) sample. Conversely, −/− and +/−, but not +/+, cDNAs were amplified by primer pair for *Neo*. Lane (w/o DNA) refers to the reaction without a template. Control amplification for the glyceraldehyde 3-phosphate dehydrogenase gene (*Gapdh*) confirms the quality of the cDNA made. (**E**) PCR genotyping of mouse tail DNA. The PCR analysis, performed on genomic DNAs derived from +/+, +/− and −/−, resulted in the amplification of the expected size fragment of wild-type allele (442 bp, upper band) in +/+ and +/− or targeted allele (152 bp, lower band) in +/− and −/−. The positions of primers are indicated in (A). M, DNA size standard.

a younger stage (2-month-old), we did not see any significant differences of seizure susceptibilities between *Efhc1* mutants and their wild-type littermates (data not shown).

Increased polysialic acid (PSA)-NCAM expression in hippocampal dentate gyri of *efhc1*-deficient mouse

Increased neurogenesis at the subgranular zone (SGZ) of the hippocampal dentate gyrus has been reported in epileptic mouse models of seizures, which are induced by chemoconvulsants or kindling (12,13). We, therefore, investigated the expression of PSA-NCAM, a marker for newly generated neurons (14), in the SGZ of 2-month-old mice without chemoconvulsant treatment. The PSA-NCAM-positive (PSA-NCAM$^+$) cells spontaneously increased in number among the heterozygous and null mutants, compared with their wild-type littermates (Fig. 4). We also performed immunohistochemistry by using anti-PSA-NCAM antibody on mouse brain sections from 2-week and 1-month-old mice. In our investigations of preliminary number of mice, we did not observe differences in the number of PSA-NCAM$^+$ cells among genotypes at these stages (data not shown). These results suggest that the increased PSA-NCAM$^+$ cell number may be induced by spontaneous seizures in the heterozygous and null mutants rather than a primary result of the *Efhc1* deficiency. Possibly, these PSA-NCAM$^+$ cells may have contributed to or further aggravated the spontaneous myoclonus and the reduction of seizure threshold in *Efhc1*-deficient mice, as previously proposed in convulsant or kindling-induced epileptic mouse models.

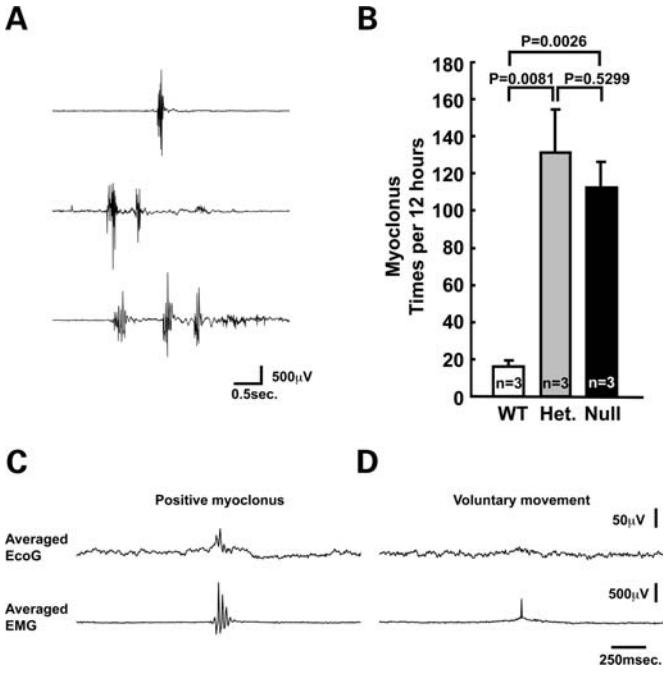

Figure 2. Increased spontaneous myoclonus in both heterozygous and null *Efhc1*-deficient mice. (**A**) Three examples of EMG recorded in null mutant mice. Quick (within 200 ms per episode) high amplitude multispikes were observed in EMG of heterozygous and null mutant mice at 7–8 months. See Supplementary Material, Video S1. (**B**) The frequency of myoclonus during 12 h in the wild-type, heterozygous and null mutant mice. The frequency of involuntary movement was seven to eight times higher in the heterozygous (131 $\pm$ 23.3 per 12 h, $P = 0.0081$) and null mutants (112.3 $\pm$ 14.1 per 12 h, $P=0.0026$), compared with the background level count of wild-type littermates (16.3 $\pm$ 3.0 per 12 h). EcoG-EMG back-averaging showed abnormal potential at spontaneous myocloni (**C**; $n = 93$) but not at voluntary movements (**D**; $n = 116$). Het, heterozygous.

Unaffected GABAergic system in *Efhc1*-deficient mouse

We also investigated functional integrities of GABA-producing interneurons in the *Efhc1* mutants. Kinetic properties of miniature inhibitory post-synaptic currents (mIPSCs) were measured from the neocortical layer II/III. Recordings were made at a holding potential of 0 mV in artificial cerebrospinal fluid (ACSF) containing tetrodotoxin. However, the mIPSCs analysis showed no differences in the amplitude, frequency, rise time or decay time in 1-month-old *Efhc1* mutants (Supplementary Material, Fig. S2). In 2-month-old mutants, increases in mIPSC frequency were observed but, again, the amplitude, rise time and decay time did not change. In keeping consistent with the results of mIPSCs, analyses of the subtype of cortical interneurons showed no differences in the numbers of parvalbumin (PV), calbindin (CB), calretinin (CR) and glutamic acid decarboxylase 67 (GAD-67) positive cells between wild-type and null mutants (Supplementary Material, Fig. S3A). The numbers of these interneurons in hippocampus were also not changed in the null mutants (data not shown). No significant changes in GAD-65/ 67 proteins in the cortex and hippocampus were noted (Supplementary Material, Fig. S3B). These results suggest that the inhibitory interneurons are mostly intact in the *Efhc1* mutants.

Enlarged brain ventricles in *Efhc1* null mutants but not in heterozygotes

Our investigations by Nissl staining of mice brain sections at 12-month-old or hematoxylin and eosin staining at post-natal day 0 (P0), P30 and 2-month-old mice revealed enlargements of ventricles in the null mutants compared with their wild-type littermates at all stages of development (Fig. 5A and B and Supplementary Material, Fig. S4A–C). The size of the hippocampus in the null mice was largely reduced, whereas the volumes of other regions were relatively conserved (ex. striatum; Supplementary Material, Fig. S4D). The ventricle enlargement was further confirmed by magnetic resonance imaging (MRI) analyses (Supplementary Material, Fig. S4E). Although enlargement of the ventricles has been reported in cases with obstruction or stricture of the aqueduct (15), the sections from the heterozygous and null *Efhc1* mutants did not show any abnormality at the aqueduct and the foramen of Monro (Fig. 5 and Supplementary Material, Fig. S4). Because of predominant expression of myoclonin1 at ependymal cilia (5), we examined the ciliary structure and measured the ciliary beat frequency (CBF) of the *Efhc1*-deficient mice. Scanning electron microscopy revealed no abnormality in the diameter and length of ependymal cilia (Fig. 6A–E). However, the CBF in the *Efhc1* null mutant mice was significantly lower when compared with the heterozygous and wild-type mice (Fig. 6F, Supplementary Material, Videos S2 and S3). This suggests that the ciliary beating defect may be the cause of ventricle enlargement in the *Efhc1* null mutant mice, as has been reported in other mice with defects of ependymal cilia (16–19).

DISCUSSION

The development of seizures and epilepsy in human JME can be categorized into three stages (20): (i) susceptibility:

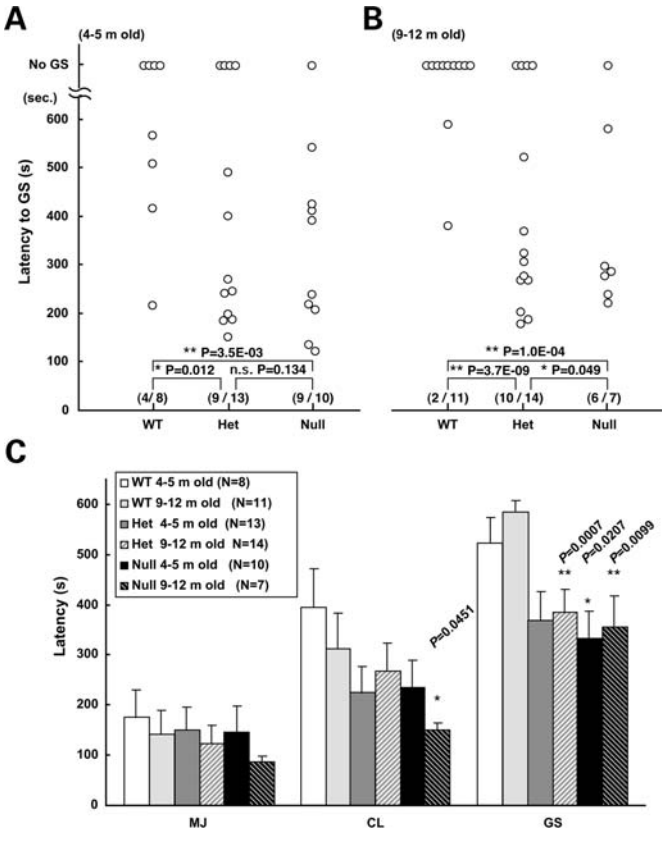

Figure 3. Increased seizure susceptibility in both heterozygous and null *Efhc1*-deficient mice. Seizure events after i.p. application of 50 mg/kg body weight of PTZ were counted. (**A** and **B**) At 4–5 months (A), percentage of animals exhibiting generalized convulsive seizures (GS) was significantly increased in heterozygous and null mutant mice. Nine of 13 (69.2%) heterozygous and 9 of 10 (90%) null mutants showed GS, whereas only 4 of 8 (50%) wild-type mice did ($n = 8–13$ per genotype). In 9–12-month-old mice (B), the percentage of animals exhibiting GS was also significantly increased in heterozygous and null mice. Ten of 14 (71.4%) heterozygous and 6 of 7 (85.7%) null mutants showed GS, whereas only 2 of 11 (18.2%) wild-type mice did ($n = 7\sim14$ per genotype). In both developmental stages, the latencies are also significantly decreased in the heterozygous and null mutants [see the histogram in (**C**)]. Open circles represent individual mice. Observation time was 600 s after drug application, and mice without GS were plotted at no GS. The numbers in round brackets indicate how many showed GS in animals tested. $^{*}P < 0.05$, $^{**}P < 0.01$. n.s., not significant. (**C**) Histogram of latencies for MJ, CL and GS in 4–5- or 9–12-month-old wild-type, heterozygous and null mutant mice with PTZ treatment ($n = 7–14$ per genotype) (see Supplementary Material, Fig. S1 for the counting of MJ and CL). For the calculation of latency periods, 600 s was temporarily assigned for the mice without seizures. In 4–5-month-old mice, the latency until onset of GS was significantly reduced in the null mutant mice (328.2 $\pm$ 53.2 s; $P = 0.0207$) compared with wild-type (512.9 $\pm$ 48.5 s). In 9–12-month-old mice, the latency until onset of GS was significantly reduced in the heterozygous (378.1 $\pm$ 45.1 s; $P = 0.0007$) and null mutant (356.4 $\pm$ 70.0 s; $P = 0.0099$) compared with wild-type (578.7 $\pm$ 20.0 s); 9–12-month-old null mice (149.6 $\pm$ 13.5 s; $P = 0.0451$) had significantly shorter latency to CL compared with wild-type (312.5 $\pm$ 70.5 s). Mean values $\pm$ SEM are shown. $^{*}P < 0.05$ and $^{**}P < 0.01$. Het, heterozygous.

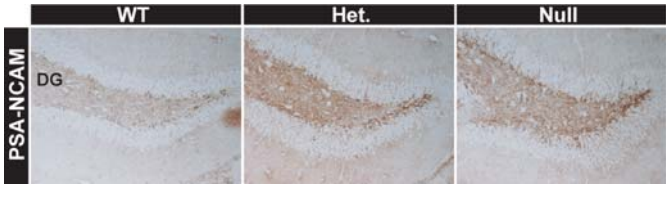

Figure 4. Increased PSA-NCAM in hippocampal dentate gyri of *Efhc1*-deficient mice. Coronal brain sections from 2-month-old mice were stained with anti-PSA-NCAM monoclonal antibody and with DAB. The expression level of PSA-NCAM in SGZ of dentate gyrus (DG) increased in the heterozygous and null mutants compared with wild-type mice. Results were reproduced in three to five mice per genotype. Het, heterozygous.

myoclonias appear mostly when triggered by fatigue, sleep deprivation, stress, menses or alcohol use. (ii) Epileptogenicity: grand mal convulsions appear 1–2 years after the first myoclonias but still need to be triggered by external stimuli. With incorrect or incomplete treatment, repeated grand mal convulsions establish the stage of epileptogenicity, in which spontaneous myoclonus and grand mal seizures start to appear. (iii) Established epileptogenesis: with more frequent spontaneous myoclonus and grand mal seizures predominating, a more enduring stage of excitability ensues and epileptogenesis is established. In this study, we found that a disruption of the *Efhc1* gene *in vivo* triggered spontaneous myoclonus and enhanced seizure susceptibility to chemoconvulsant, providing evidence that the reduction or loss of function of myoclonin1 causes epilepsy. The *Efhc1*-deficient mice are developmentally normal and fertile, but developed spontaneous myoclonus at adult stages. At 4–12 months of age, the heterozygous and null mutants showed enhanced seizure susceptibility to PTZ stimulation. Thus, *Efhc1* heterozygous and null mutant mice replicate the developmental stage dependency of susceptibility in human JME. However, a number of

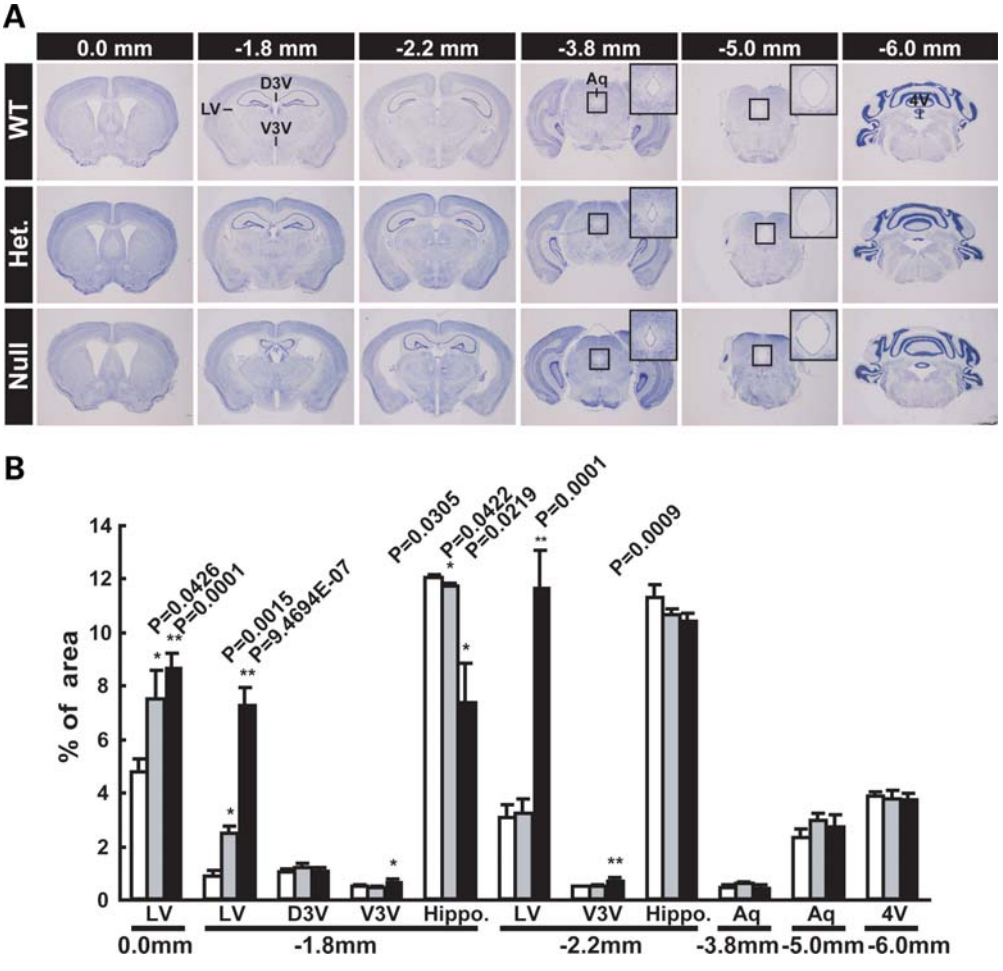

Figure 5. Enlarged brain ventricles in *Efhc1* null mutants but not in heterozygotes. (**A**) Nissl staining of serial coronal sections of brains from 12-month-old mice. Distances from bregma are shown above. Insets are higher magnifications of aqueducts. Het, heterozygous. (**B**) The sizes of the ventricle and hippocampal areas on the Nissl-stained sections were calculated by the NIH image software ($n = 3$ per genotype). Significant enlargement of lateral ventricles (LV) and decreased volume of hippocampus were observed in the null mutants compared with wild-type littermates ($P = 9.4694\text{E}-07$–0.0001 at 0.0 to -2.2 mm from bregma). The third ventricle was also significantly enlarged in the null mutants (-1.8 to -2.2 mm from bregma). Enlargement of the ventricles in the heterozygotes was very mild (LV at 0.0 and -1.8 mm) or mostly not observed (LV at -2.2 mm). The sections from heterozygous and null mice did not show noticeable abnormalities at the aqueduct and fourth ventricle (-3.8 to -6.0 mm from bregma). LV, lateral ventricle; D3V, dorsal third ventricle; V3V, ventral third ventricle; Aq, aqueduct; 4V, fourth ventricle. White bars, wild-type; grey bars, heterozygotes; blackened bars, null mutants.

different mouse epilepsy models with gene knockouts do not show spontaneous or handling-induced tonic-CL until they are >2 months of age. Therefore, at present, it would be too early to conclude that the 'stage dependence' is an *EFHC1*-specific feature. Furthermore, the mutant mice do not develop tonic-CLs, absence seizures and spike-wave complexes that have been reported in patients with JME. This may suggest that additional (environmental, genetic, or species-specific) factors contribute to the appearance of tonic-CLs and absence seizures in humans.

How does the impairment of myoclonin1 cause epilepsy? It has been proposed that the ciliary defects in patients with *EFHC1* mutations may cause abnormal CSF flow, which can lead to abnormal neural migration and result in epilepsy (21). However, in our study, ventricle enlargement possibly caused by the ciliary beating defect was minor or mostly not observed in the heterozygous *Efhc1*-deficient mouse. Still, these heterozygotes showed frequent spontaneous myoclonus and enhanced seizure susceptibility to PTZ stimulation, mostly similar to that of *Efhc1* null mutant. These observations suggest that the ventricle enlargement and the ciliary beating defect themselves may not be directly relevant to myoclonus and enhanced seizure susceptibility observed in *Efhc1*-deficient mice. In addition, the size of hippocampus in the null mutant mice was largely reduced, but this reduction in size was not observed in heterozygotes. The reduction also did not correlate with the epileptic phenotype in heterozygotes, and therefore, the hippocampal size reduction may not be directly relevant to the epileptic phenotypes. For the moment, it is still very difficult to speculate on the pathological cascade in the mice and that of *EFHC1* mutation-dependent epilepsy in patients as well. However, if any phenotypic parameters (ex. CSF secretion from choroid plexus, ion exchange at ependymal cell or pH of CSF) that are abnormal in both the heterozygous and null *Efhc1* mutants can be identified, it may indicate that one or all of those parameters are most likely the basis for the epileptic seizure phenotypes.

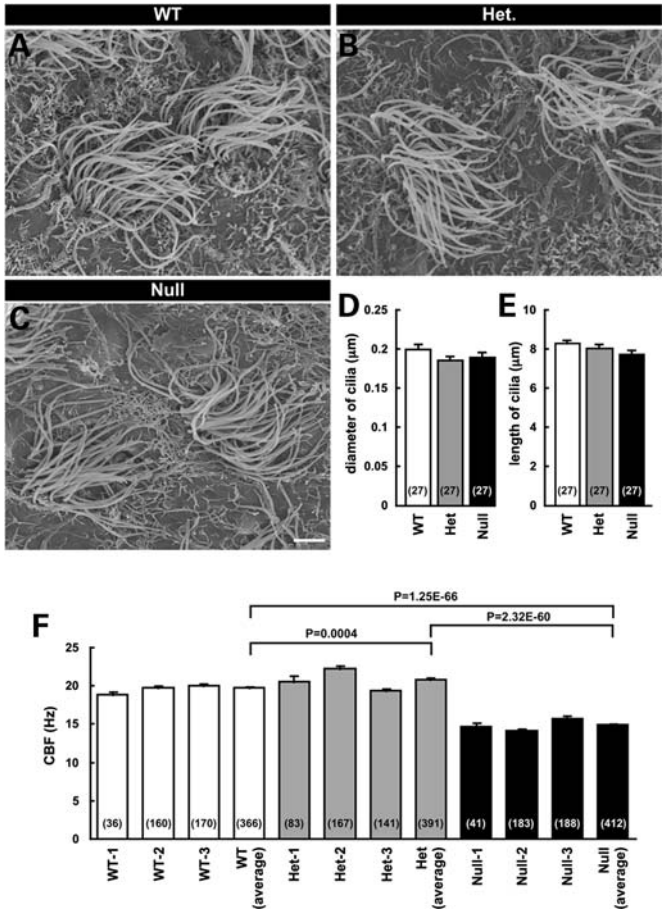

Figure 6. Unaffected morphology but affected motility of ependymal cilia in *Efhc1*-deficient mice. (**A**–**C**) Electron microscopic images of ependymal cilia on the lateral ventricle walls of the wild-type, heterozygous and null mutant mice at 3 months. No significant difference was observed in the diameter (**D**) and length (**E**) of the cilia (means ± SEM) among genotypes. Scale bar: 2 μm. (**F**) The CBF in the null mutant mice was significantly low (14.90 ± 0.21 Hz) compared with that of heterozygous (20.85 ± 0.26 Hz) and wild-type (19.80 ± 0.15 Hz). CBFs were measured in 412 cells from three null mutants, 391 cells from three heterozygous and 366 cells from three wild-type mice at 8–13 months. See Supplementary Material, Videos S2 and S3. The numbers in round brackets indicate how many cilia (D, E) and cells (F) were measured. Het, heterozygous.

We reported earlier that myoclonin1 co-localized and interacted specifically with the R-type calcium channel, $Ca_v2.3$, in neurons, and increased R-type Ca^{2+} current generated this channel (4). However, in our recent study with a newly generated anti-myoclonin1 monoclonal antibody and by using *Efhc1*-deficient mice as a negative control, we revealed that the mouse myoclonin1 protein was not observed in neuronal cells, but dominantly expressed in the embryonic choroid plexus and post-natal ependymal cilia (5). Another group reported that the myoclonin1 was localized at mitotic spindle in cultured cell lines and proposed that myoclonin1 could play an important role during cell division (22), but so far our previously mentioned anti-myoclonin1 monoclonal antibody did not detect any signals in the mitotic spindle structure (unpublished data). It is, however, still possible that the affinity of our anti-myoclonin1 monoclonal antibody may not be high enough to detect lower levels of myoclonin1 expression in the neuronal cells or at the mitotic spindle structure. Alternatively, our anti-myoclonin1 monoclonal antibody may not be able to bind to altered epitopes found in different myoclonin1 isoforms, which may possibly be expressed in neurons or the mitotic spindle. Further, careful investigation on the tissue or subcellular distribution of myoclonin1 protein is apparently required to fully elucidate the spatial expression of myoclonin1 and its various isoforms.

To date, most of genes responsible for idiopathic epilepsies have been identified (~20 genes) as ion channels (23–32). However, with the exception of sodium channel type I alpha subunit, *SCN1A*, in severe myoclonic epilepsy of Dravet (29), ion channel mutations have been unique to no more than a few of specific families. Therefore, it could be mentioned that genes responsible for most patients with idiopathic epilepsies remain unidentified. In contrast to the epileptic ion channel genes, multiple mutations of *EFHC1*, encoding the non-ion channel protein myoclonin1, have been described in multiple idiopathic epilepsies. The investigations of the molecular mechanism for epilepsies caused by *EFHC1* mutations may reveal novel pathological cascades and should greatly contribute to the understanding of epilepsy as a whole.

About 60% of the patients with JME were free from all seizure types (grand mal, myoclonic and absence seizures) during anti-epileptic drug treatment, but these seizures

continued in 40% of the patients despite drug treatment (20). Currently, there is no completely effective treatment for JME. To develop a more effective treatment for JME, additional studies are required to understand the mechanism of developing myoclonus and reducing seizure threshold by alteration of myoclonin1. Our *Efhc1*-deficient mice may enable further studies for discovery of therapeutic targets, developing a more effective treatment and perhaps eventually finding a cure for JME.

In summary, we observed frequent spontaneous myoclonus and increased seizure susceptibility in mice with *Efhc1* deficiency. These results replicate the stage of susceptibility in human JME and further support our contention that reduction or loss of function of myoclonin1 leads to enhanced susceptibility and epileptogenicity in patients with *EFHC1* mutations.

MATERIALS AND METHODS

Generation of *Efhc1*-deficient mice

All experimental protocols were approved by the Animal Experiment Committee of RIKEN Brain Science Institute. A genomic clone of the murine *Efhc1* gene was isolated from RPCI-22 129s6/SvEvTAC Taconic (F) BAC library segment 2 (BACPAC Resource Center). A 5.7 kb *Bam*HI/*Xho* I fragment including the *Efhc1* exon 1 sequence was cloned into pBluescript SK (−) (Stratagene). A neomycin selection marker, loxP-pgk-neo-loxP cassette, was inserted into *Sma* I site in *Efhc1* exon 1. A 1.1 kb MC1-DT-A cassette (a generous gift from Dr Yagi, Osaka University, Osaka, Japan), a negative selection marker, was added at the 3′-end of the targeting vector. The targeting vector linearized with *Kpn* I was electroporated into approximately 5×10^7 E14 ES cells with a Gene-Pulser (Bio-Rad Laboratories) at 3 μF and 800 V. Transfected cells were plated on neomycin-resistant, mitomycin C-treated mouse embryonic feeder (MEF) cells in 10 cm dishes. One day after plating, positive selection was performed in the presence of Geneticin (G418; 150 μg/ml). Resistant clones were picked at days 8–10 and subsequently expanded into 96-well plates pre-seeded with MEF. *Hin*dIII-digested genomic DNA from individual clones was analyzed by Southern blot, with a 956 bp probe derived from the genomic sequence immediately downstream of the targeting vector (probe-R). The probe-R was generated by PCR using primers 5′-TTCTACAAGTGTGGGTAGGAGTG-3′ and 5′-CTGCTCTGTGATGTCCGATT-3′. Positive clones were further confirmed by PCR using primers 1 (5′-GCTCAGTTCAGCCTTAAAGTTG-3′) and 2 (5′-CCACTTGTGTAGCGCCAA-3′). Homologous recombinant ES cells from each of the six targeted clones were injected into mouse C57BL/6J (B6J) blastocysts. Two ES clones (8G and 9A) produced several chimeras. Chimeric male mice were mated with B6J females to generate KO-*Efhc1*-B6J mice. The heterozygous mice were further crossbred with B6J mice four to eight times, and the resultant heterozygous mice were interbred to obtain the wild-type, heterozygous and homozygous mice. Genotypes were determined by PCR. The following PCR primers were used: primer 3 (5′-AGTTTGTTGCCAGGGTAACC-3′), primer 4 (5′-TGAGGATTCAGAAGCGGTG-3′), primer 5 (5′-TGAATGAACTGCAGGACGAGG-3′) and primer 6 (5′-AAGGTGAGATGACAGGAGATC-3′) (Fig. 1A). Primers 3 and 4 yield 442 bp fragments from the wild-type allele, and primers 5 and 6 yield 152 bp fragments from the mutant allele.

RT–PCR

Brain, kidney and liver tissues were dissected from post-natal (P) 24 days mice, and RNA was extracted and first-strand cDNA was obtained as described previously (4). To amplify mouse cDNA, we designed primers on *Efhc1* exons 1 and 3, *neomycin* and g*apdh*. Primer sequences are available upon request.

Electrocorticographic (EcoG) and EMG recordings

Recordings of EcoG and EMG were performed with 7–8-month-old wild-type, heterozygous and null mice ($n = 3$, each genotype). Stainless steel screws (1.1 mm diameter) that served as EcoG electrode were implanted over the somatosensory cortex (1.5 mm lateral to midline, 1.0 mm posterior to bregma) under 1.5% halothane anesthesia with N_2O:O_2 (3:2) ventilation in 1 week before recording. An indifferent electrode was implanted on the cerebellum (at midline, 2.0 mm posterior to lambda) as ground electrode. Two stainless steel wires (0.1 mm diameter, 1.3 mm distance) that served as bipolar-type EcoG electrode were also implanted over the somatosensory cortex. EMG electrodes were placed 2–3 mm apart from the cervical region of the trapezius muscle.

Seizure susceptibility

PTZ (Sigma) dissolved in 1× phosphate-buffered saline (PBS) was administered i.p. at a dose of 50 mg/kg body weight in a total volume of 200–300 μl. After injection, the animals were watched closely for 10 min. The latency of until onset of twitch, repeated CL or fully generalized seizure was measured.

Histological analysis

Mice (P0 upto 12-month-old) were perfused intracardially with 4% paraformaldehyde (PFA) in 1× PBS (pH 7.4) at 4°C. Preparations of mouse brain sections (paraffin or frozen), staining of sections (Nissl and hematoxylin-eosin) and immunohistochemical staining were carried out as described previously (5,33). The following antibodies were used: anti-PSA-NCAM antibody (1:500; Chemicon), anti-PV antibody (1:2000; Swant), anti-CB antibody (1:500; Chemicon), anti-CR antibody (1:2000; Swant) and anti-GAD-67 antibody (1:4000; Chemicon). Immunoreactivity was visualized using a Vectastain ABC kit (Vector Laboratories), developed with ImmunoPure Metal-enhanced diaminobenzidine (DAB) Substrate Kit (Pierce). Areas of the ventricles and hippocampus of Nissl-stained sections were determined using NIH image software (ImageJ).

Scanning electron microscopy

Freshly isolated brains from wild-type, heterozygous and null mice were processed for scanning electron microscopy as described previously (34). The entire lateral wall of the lateral ventricles was dissected and fixed with 2.5% glutaraldehyde/2% PFA for overnight. The tissues were incubated in 2% OsO_4 for 1 h, dehydrated with ethanol and dried with a critical point drier. After sputter coating with platinum, the mounted samples were examined with a scanning electron microscope (HITACHI S-5000).

Measurement of CBF

The brains were removed from anesthetized mice, and the surface of the lateral and fourth ventricles was cut into small pieces in HCO_3^- solution at 4°C. The HCO_3^- solution had the following composition (in millimolar): 121 NaCl, 4.5 KCl, 1 $MgCl_2$, 1.5 $NaHCO_3$, 1.5 $CaCl_2$, 1.5 NaHEPES, 5 HEPES and 5 glucose. The tissue block was cut into thin pieces by two adherent razor blades and was placed on a cover slip pre-coated with Cell-Tak (Becton–Dickinson Labware) to adhere slices firmly on the cover slip. The cover slip with slices was set in the perfusion chamber, the volume of which was 20 μl, and the rate of perfusion was 200 μl/min. The chamber was mounted on a differential interference contrast microscope (E600-FN; Nikon), which was connected to a high-speed digital video camera (FASTCAM 512PCI; Photoron). The sampling rate of the high-speed camera was 500 Hz. The CBF was calculated from the time for 10 beating cycles.

Electrophysiology

Acute brain slices were prepared from wild-type and null mice at 1 and 2 months. Briefly, the mice were decapitated, and the brain was rapidly removed from ice-cold oxygenated ACSF. Coronal slices of the somatosensory cortex (300 μm thick) were obtained using a tissue slicer (Vibratome 3000; Vibratome) in 4°C oxygenated ACSF. Slices were placed in an incubating chamber of oxygenated ACSF at 31°C for at least 1 h before recording. ACSF had the following composition (in millimolar): 124 NaCl, 3 KCl, 1.25 NaH_2PO_4, 1 $MgSO_4$, 26 $NaHCO_3$, 2 $CaCl_2$ and 10 glucose. The ACSF was bubbled continuously with 95% O_2–5% CO_2. Whole-cell voltage-clamp recordings were obtained from visually identified neurons using an infrared differential interference contrast (IR-DIC) microscopy system. Patch electrodes (3–5 MΩ) were pulled from borosilicate glass capillary tubing and fire polished. Intracellular patch pipette solution contained (in millimolar) 130 Cs-gluconate, 10 HEPES, 8 KCl, 10 Na-phosphocreatine, 3 QX314, 4 Na_2-ATP and 0.5 Na_2-GTP, pH 7.25 (285–290–mOsm). To isolate GABAergic currents, slices were perfused with ACSF containing either 20 μM 6-ciano-7-dinitroquinoxaline-2,3-dione (CNQX) or 50 μM D-(−)-2-amino-5-phosphonovaleric acid (D-AP5). Whole-cell voltage-clamp data were low-pass filtered at 1 kHz (−3 dB, eight-pole Bessel), digitally sampled at 10 kHz and monitored with Igor 4.1 software (WaveMetric Inc.). Whole-cell access resistance was carefully monitored throughout the recording, and cells were rejected if values changed by >15%; only recordings with stable series resistance of <30 MΩ were used for analysis. Each event was manually selected on the basis of rise time, amplitude and decay properties. Between 500 and 800 individual events were analyzed for each cell with the Mini Analysis program (Synaptosoft). We considered all recorded events in a single experiment for the determination of mice.

Western blot analysis

Preparations of mouse brain protein samples and western blot analyses were performed as described previously (4). The following antibodies were used: anti-GAD-65/ 67 (Biomol), 1:4000 dilution or anti-GAPDH (Santa Cruz), 1:1000 dilution. A horseradish peroxidase (HRP)-conjugated anti-mouse IgG (1:3000, Promega) or HRP-conjugated anti-rabbit IgG (1:1000, Santa Cruz) was used for secondary antibody.

High resolution MRI

Mice were anesthetized with pentobarbital and subjected to micro-MRI scans using a vertical bore 9.4 T Bruker AVANCE 400WB imaging spectrometer with a 250 mTm^{-1} actively shielded microimaging gradient insert (Bruker BioSpin) (35). A 25 mm resonator was used for signal excitation and detection. The depth of anesthesia was monitored with a breathing sensor and was maintained with 0.5–1.5% isoflurane in air. The T1-weighted MRI scans were performed with the following imaging parameters: matrix size = 256 × 256 and number of slices: 15. The T2-weighted MRI scans were performed with the following imaging parameters: matrix size = 256 × 512; TR: 3000 ms; slice thickness = 0.5 mm; number of slices: 32 and total imaging time: 100 min (four averages).

Statistical analysis

All data were expressed as mean ± SEM. The significance of differences between mean values was assessed by two-tailed Student's *t*-tests or χ^2 test, with $P < 0.05$ taken to indicate statistical significance.

SUPPLEMENTARY MATERIAL

Supplementary Material is available at *HMG* online.

ACCESSION NUMBERS

Human EFHC1 isoforms: EU520261 (long) and AY608690 (short), mouse Efhc1: EU520262 (NCBI, Entrez Nucleotide). Human myoclonin1 isoforms: ACB20691 (long) and AAT67419 (short), mouse myoclonin1: ACB20692 (NCBI, Entrez Protein).

ACKNOWLEDGEMENTS

We would like to thank Susumu Ito, Tojo Nakayama, Mika Tanaka, Chieko Nishioka, Nami Okamura and Emi Mazaki

for their helpful discussions and comments on the manuscript or technical assistance. We also thank Andrew W. Liu for his comments and for editing of the manuscript. We are indebted to the Research Resources Center of RIKEN Brain Science Institute (BSI) for DNA sequencing analysis, knockout mice production services and tissue section services.

Conflict of Interest statement. The authors declare no competing financial interest.

FUNDING

This work was supported in part by a grant from RIKEN Brain Science Institute (K.Y.), from the Ministry of Education, Culture, Sports, Science and Technology of Japan (T.S.) and from RIKEN Special Postdoctoral Researchers Program (T.S.).

REFERENCES

1. Delgado-Escueta, A.V. and Enrile-Bacsal, F. (1984) Juvenile myoclonic epilepsy of Janz. *Neurology*, **34**, 285–294.
2. Nicoletti, A., Reggio, A., Bartoloni, A., Failla, G., Sofia, V., Bartalesi, F., Roselli, M., Gamboa, H., Salazar, E., Osinaga, R. *et al.* (1999) Prevalence of epilepsy in rural Bolivia: a door-to-door survey. *Neurology*, **53**, 2064–2069.
3. Panayiotopoulos, C.P., Obeid, T. and Tahan, A.R. (1994) Juvenile myoclonic epilepsy: a 5-year prospective study. *Epilepsia*, **35**, 285–296.
4. Suzuki, T., Delgado-Escueta, A.V., Aguan, K., Alonso, M.E., Shi, J., Hara, Y., Nishida, M., Numata, T., Medina, M.T., Takeuchi, T. *et al.* (2004) Mutations in EFHC1 cause juvenile myoclonic epilepsy. *Nat. Genet.*, **36**, 842–849.
5. Suzuki, T., Inoue, I., Yamagata, T., Morita, N., Furuichi, T. and Yamakawa, K. (2008) Sequential expression of Efhc1/myoclonin1 in choroid plexus and ependymal cell cilia. *Biochem. Biophys. Res. Commun.*, **367**, 226–233.
6. Ikeda, T., Ikeda, K., Enomoto, M., Park, M.K., Hirono, M. and Kamiya, R. (2005) The mouse ortholog of EFHC1 implicated in juvenile myoclonic epilepsy is an axonemal protein widely conserved among organisms with motile cilia and flagella. *FEBS Lett.*, **579**, 819–822.
7. Ma, S., Blair, M.A., Abou-Khalil, B., Lagrange, A.H., Gurnett, C.A. and Hedera, P. (2006) Mutations in the GABRA1 and EFHC1 genes are rare in familial juvenile myoclonic epilepsy. *Epilepsy Res.*, **71**, 129–134.
8. Annesi, F., Gambardella, A., Michelucci, R., Bianchi, A., Marini, C., Canevini, M.P., Capovilla, G., Elia, M., Buti, D., Chifari, R. *et al.* (2007) Mutational analysis of EFHC1 gene in Italian families with juvenile myoclonic epilepsy. *Epilepsia*, **48**, 1686–1690.
9. Stogmann, E., Lichtner, P., Baumgartner, C., Bonelli, S., Assem-Hilger, E., Leutmezer, F., Schmied, M., Hotzy, C., Strom, T.M., Meitinger, T. *et al.* (2006) Idiopathic generalized epilepsy phenotypes associated with different EFHC1 mutations. *Neurology*, **67**, 2029–2031.
10. Medina, M.T., Suzuki, T., Alonso, M.E., Duron, R.M., Martinez-Juarez, I.E., Bailey, J.N., Bai, D., Inoue, Y., Yoshimura, I., Kaneko, S. *et al.* (2008) Novel mutations in myoclonin1/EFHC1 in sporadic and familial juvenile myoclonic epilepsy. *Neurology*, **70**, 2137–2144.
11. Huang, R.Q., Bell-Horner, C.L., Dibas, M.I., Covey, D.F., Drewe, J.A. and Dillon, G.H. (2001) Pentylenetetrazole-induced inhibition of recombinant gamma-aminobutyric acid type A (GABA(A)) receptors: mechanism and site of action. *J. Pharmacol. Exp. Ther.*, **298**, 986–995.
12. Parent, J.M., Yu, T.W., Leibowitz, R.T., Geschwind, D.H., Sloviter, R.S. and Lowenstein, D.H. (1997) Dentate granule cell neurogenesis is increased by seizures and contributes to aberrant network reorganization in the adult rat hippocampus. *J. Neurosci.*, **17**, 3727–3738.
13. Parent, J.M., Elliott, R.C., Pleasure, S.J., Barbaro, N.M. and Lowenstein, D.H. (2006) Aberrant seizure-induced neurogenesis in experimental temporal lobe epilepsy. *Ann. Neurol.*, **59**, 81–91.
14. Fanarraga, M.L., Avila, J. and Zabala, J.C. (1999) Expression of unphosphorylated class III beta-tubulin isotype in neuroepithelial cells demonstrates neuroblast commitment and differentiation. *Eur. J. Neurosci.*, **11**, 516–527.
15. Mashayekhi, F., Draper, C.E., Bannister, C.M., Pourghasem, M., Owen-Lynch, P.J. and Miyan, J.A. (2002) Deficient cortical development in the hydrocephalic Texas (H-Tx) rat: a role for CSF. *Brain*, **125**, 1859–1874.
16. Taulman, P.D., Haycraft, C.J., Balkovetz, D.F. and Yoder, B.K. (2001) Polaris, a protein involved in left–right axis patterning, localizes to basal bodies and cilia. *Mol. Biol. Cell*, **12**, 589–599.
17. Takaki, E., Fujimoto, M., Nakahari, T., Yonemura, S., Miyata, Y., Hayashida, N., Yamamoto, K., Vallee, R.B., Mikuriya, T., Sugahara, K. *et al.* (2007) Heat shock transcription factor 1 is required for maintenance of ciliary beating in mice. *J. Biol. Chem.*, **282**, 37285–37292.
18. Davis, R.E., Swiderski, R.E., Rahmouni, K., Nishimura, D.Y., Mullins, R.F., Agassandian, K., Philp, A.R., Searby, C.C., Andrews, M.P., Thompson, S. *et al.* (2007) A knockin mouse model of the Bardet–Biedl syndrome 1 M390R mutation has cilia defects, ventriculomegaly, retinopathy, and obesity. *Proc. Natl Acad. Sci. USA*, **104**, 19422–19427.
19. Lechtreck, K.F., Delmotte, P., Robinson, M.L., Sanderson, M.J. and Witman, G.B. (2008) Mutations in Hydin impair ciliary motility in mice. *J. Cell Biol.*, **180**, 633–643.
20. Martinez-Juarez, I.E., Alonso, M.E., Medina, M.T., Duron, R.M., Bailey, J.N., Lopez-Ruiz, M., Ramos-Ramirez, R., Leon, L., Pineda, G., Castroviejo, I.P. *et al.* (2006) Juvenile myoclonic epilepsy subsyndromes: family studies and long-term follow-up. *Brain*, **129**, 1269–1280.
21. King, S.M. (2006) Axonemal protofilament ribbons, DM10 domains, and the link to juvenile myoclonic epilepsy. *Cell Motil. Cytoskeleton*, **63**, 245–253.
22. de Nijs, L., Lakaye, B., Coumans, B., Leon, C., Ikeda, T., Delgado-Escueta, A.V., Grisar, T. and Chanas, G. (2006) EFHC1, a protein mutated in juvenile myoclonic epilepsy, associates with the mitotic spindle through its N-terminus. *Exp. Cell Res.*, **312**, 2872–2879.
23. Singh, N.A., Charlier, C., Stauffer, D., DuPont, B.R., Leach, R.J., Melis, R., Ronen, G.M., Bjerre, I., Quattlebaum, T., Murphy, J.V. *et al.* (1998) A novel potassium channel gene, KCNQ2, is mutated in an inherited epilepsy of newborns. *Nat. Genet.*, **18**, 25–29.
24. Charlier, C., Singh, N.A., Ryan, S.G., Lewis, T.B., Reus, B.E., Leach, R.J. and Leppert, M. (1998) A pore mutation in a novel KQT-like potassium channel gene in an idiopathic epilepsy family. *Nat. Genet.*, **18**, 53–55.
25. Wallace, R.H., Wang, D.W., Singh, R., Scheffer, I.E., George, A.L. Jr, Phillips, H.A., Saar, K., Reis, A., Johnson, E.W., Sutherland, G.R. *et al.* (1998) Febrile seizures and generalized epilepsy associated with a mutation in the Na+-channel beta1 subunit gene SCN1B. *Nat. Genet.*, **19**, 366–370.
26. Escayg, A., MacDonald, B.T., Meisler, M.H., Baulac, S., Huberfeld, G., An-Gourfinkel, I., Brice, A., LeGuern, E., Moulard, B., Chaigne, D. *et al.* (2000) Mutations of SCN1A, encoding a neuronal sodium channel, in two families with GEFS+2. *Nat. Genet.*, **24**, 343–345.
27. Wallace, R.H., Marini, C., Petrou, S., Harkin, L.A., Bowser, D.N., Panchal, R.G., Williams, D.A., Sutherland, G.R., Mulley, J.C., Scheffer, I.E. *et al.* (2001) Mutant GABA(A) receptor gamma2-subunit in childhood absence epilepsy and febrile seizures. *Nat. Genet.*, **28**, 49–52.
28. Baulac, S., Huberfeld, G., Gourfinkel-An, I., Mitropoulou, G., Beranger, A., Prud'homme, J.F., Baulac, M., Brice, A., Bruzzone, R. and LeGuern, E. (2001) First genetic evidence of GABA(A) receptor dysfunction in epilepsy: a mutation in the gamma2-subunit gene. *Nat. Genet.*, **28**, 46–48.
29. Claes, L., Del-Favero, J., Ceulemans, B., Lagae, L., Van Broeckhoven, C. and De Jonghe, P. (2001) *De novo* mutations in the sodium-channel gene SCN1A cause severe myoclonic epilepsy of infancy. *Am. J. Hum. Genet.*, **68**, 1327–1332.
30. Sugawara, T., Tsurubuchi, Y., Agarwala, K.L., Ito, M., Fukuma, G., Mazaki-Miyazaki, E., Nagafuji, H., Noda, M., Imoto, K., Wada, K. *et al.* (2001) A missense mutation of the Na+ channel alpha II subunit gene Na(v)1.2 in a patient with febrile and afebrile seizures causes channel dysfunction. *Proc. Natl Acad. Sci. USA*, **98**, 6384–6389.
31. Cossette, P., Liu, L., Brisebois, K., Dong, H., Lortie, A., Vanasse, M., Saint-Hilaire, J.M., Carmant, L., Verner, A., Lu, W.Y. *et al.* (2002) Mutation of GABRA1 in an autosomal dominant form of juvenile myoclonic epilepsy. *Nat. Genet.*, **31**, 184–189.
32. Haug, K., Warnstedt, M., Alekov, A.K., Sander, T., Ramirez, A., Poser, B., Maljevic, S., Hebeisen, S., Kubisch, C., Rebstock, J. *et al.* (2003) Mutations in CLCN2 encoding a voltage-gated chloride channel are

associated with idiopathic generalized epilepsies. *Nat. Genet.*, **33**, 527–532.
33. Ogiwara, I., Miyamoto, H., Morita, N., Atapour, N., Mazaki, E., Inoue, I., Takeuchi, T., Itohara, S., Yanagawa, Y., Obata, K. *et al.* (2007) Na(v)1.1 localizes to axons of parvalbumin-positive inhibitory interneurons: a circuit basis for epileptic seizures in mice carrying an Scn1a gene mutation. *J. Neurosci.*, **27**, 5903–5914.
34. Sawamoto, K., Wichterle, H., Gonzalez-Perez, O., Cholfin, J.A., Yamada, M., Spassky, N., Murcia, N.S., Garcia-Verdugo, J.M., Marin, O., Rubenstein, J.L. *et al.* (2006) New neurons follow the flow of cerebrospinal fluid in the adult brain. *Science*, **311**, 629–632.
35. Higuchi, M., Iwata, N., Matsuba, Y., Sato, K., Sasamoto, K. and Saido, T.C. (2005) 19F and 1H MRI detection of amyloid beta plaques *in vivo*. *Nat. Neurosci.*, **8**, 527–533.